J. Plasma Phys. (2025), *vol*. 91, E37
Published by Cambridge University Press

doi:10.1017/S0022377824001727

On heat conduction in a plasma with a magnetic island

G. Pechstein [1],†, **P. Helander** [1] **and B. Shanahan** [1]

[1]Stellarator Theory, Max-Planck-Institut für Plasmaphysik, Wendelsteinstraße 1, 17491 Greifswald, Germany

(Received 22 May 2024; revised 17 December 2024; accepted 18 December 2024)

The heat conductivity of a plasma is usually much higher along the magnetic field than across it, and, as a result, the presence of a magnetic island can significantly affect the temperature profile in its vicinity. Radiation energy losses, which depend sensitively on temperature, are thus strongly affected by magnetic islands. This phenomenon is explored in a simple mathematical setting, and it is shown that the presence of a magnetic island greatly enhances a plasma's capacity to radiate energy. In the limit of highly anisotropic heat conductivity, the steady-state heat conduction equation can be reduced to an ordinary differential equation. Although this equation operates in one dimension, the topology is not that of the real line, but corresponds to a rod with a cooling fin. As parameters such as the incoming heat flux or the radiation amplitude are varied, the radiation has a tendency to linger around the island, in particular in the region of the separatrix, and the total radiated energy is then significantly increased. The island acts as a 'cooling fin' to the plasma. Furthermore, the solutions exhibit bifurcations, where the location of the radiation zone suddenly changes.

Key words: plasma devices, plasma simulation, plasma confinement

1. Introduction

In magnetically confined fusion plasmas, energy is transported across flux surfaces towards the plasma edge and the surrounding vessel. It is a challenge to control and limit the wall loads since the tolerable energy flux onto a plasma facing component is limited by a number of technical constraints. In order to control and reduce the loads, tokamaks and stellarators exploit divertor magnetic fields (König *et al.* 2002; Feng *et al.* 2011) to guide the heat flux onto target plates, and try to maximise radiation from the edge plasma. When the radiative losses are particularly high, the plasma sometimes 'detaches' from the walls and the energy flux to the latter drops dramatically (Jakubowski *et al.* 2021).

The key feature of plasma energy transport that allows for the use of a divertor is the fact that the transport is highly anisotropic. Insofar as the heat flux is diffusive, the conductivity is many orders of magnitude higher in the direction along the magnetic field than across it. As a result, if the magnetic field is shaped in such a way that different field lines have

† Email address for correspondence: gregor.pechstein@ipp.mpg.de

different topologies, the heat flux can vary greatly across any surface across which the topology changes. The most familiar example is the separatrix at the tokamak edge, which separates closed magnetic surfaces in the confinement region from the scrape-off layer with field lines that intersect the first wall. The W7-X stellarator uses a different kind of divertor, where a chain of four to six magnetic islands function as a scrape-off layer directing the plasma to divertor target plates. Energy is removed from the plasma by two mechanisms. One the one hand, the target plates constitute a heat sink on all intersected field lines, and on the other hand radiative cooling from impurity ions such as carbon remove thermal energy from the plasma. Transport computations in the specific geometry of W7-X and other stellarators are routinely carried out with the EMC3-EIRENE code in order to quantify these energy loss mechanisms (Feng *et al.* 2021).

In the present paper, we take a more academic approach and consider the anisotropic heat conduction and radiation in the simplest possible mathematical setting in which the field lines change topology, namely, in the geometry of a single chain of magnetic islands. The aim is to shed light on the basic question of how a variation in field-line topology affects the location and amount of plasma radiation. As we shall see, even when reduced to this simple form, the problem is surprisingly complex and allows for highly non-trivial behaviour. In particular, we find that the plasma has a propensity of radiating in the vicinity of the magnetic island and its immediate vicinity, and that bifurcated solutions are possible.

The mathematical equation we solve is a two-dimensional (2-D) heat conduction equation with a loss term. In the literature, many other studies of such equations in the context of tokamak edge transport exist. For instance, Krasheninnikov (1997) and Krasheninnikov, Batishcheva & Simakov (1998) considered the same equation as we did for the purpose of exploring effects of the magnetic-field geometry on radiation fronts and their stability, while Paul, Hudson & Helander (2022) analysed the properties of a 2-D heat conduction equation in an island geometry without a loss term.

The rest of the paper is structured as follows. The next section is devoted to the reduction of the three-dimensional (3-D) heat conduction equation to a one-dimensional (1-D) form in the limit of high anisotropy. In § 3, we compute the effective heat conduction coefficient in the geometry of a magnetic field with a simple island, before solving the equation including a radiation loss term in § 5. Section 6 summarises the results.

2. Anisotropic heat conduction

We proceed from an anisotropic heat conduction equation, with a temperature-dependent sink that models radiation losses in and around a magnetic island. As we shall see, the full 3-D heat conduction equation can, in the limit of highly anisotropic heat conductivity, be reduced to an ordinary differential equation. This reduction is achieved by flux-surface averaging the heat conduction equation, and results in a 1-D description with an effective heat conduction coefficient that carries information about the magnetic geometry.

We consider a heat conduction equation of the form

$$\nabla \cdot \boldsymbol{q} + R(T) = 0, \tag{2.1}$$

where $\boldsymbol{q}$ denotes the heat flux and $R(T)$ the energy loss due to radiation, which depends on the temperature T. For simplicity we ignore any dependence on density, and assume that the plasma is optically thin to the radiation, so that the latter simply acts as an energy sink. In the classical theory of collisional transport in magnetised plasmas (Braginskii 1965; Helander & Sigmar 2005), the electron heat flux is equal to

$$\boldsymbol{q} = -\kappa_\parallel \nabla_\parallel T - \kappa_\wedge \boldsymbol{b} \times \nabla T - \kappa_\perp \nabla_\perp T, \tag{2.2}$$

https://doi.org/10.1017/S0022377824001727 Published online by Cambridge University Press

where T is the electron temperature, $\boldsymbol{b} = \boldsymbol{B}/B$ a unit vector pointing in the direction of the magnetic field, $\nabla_\parallel = \boldsymbol{bb} \cdot \nabla$, and $\nabla_\perp T = \nabla T - \boldsymbol{bb} \cdot \nabla T$. The three different heat conductivities that appear in this relation are of very different magnitude in a strongly magnetised plasma. Heat conduction is far more effective in the direction along the field than in the two directions perpendicular to it, so we adopt the ordering

$$\kappa_\parallel \gg \kappa_\wedge \sim \kappa_\perp. \tag{2.3}$$

In Braginskii's theory, the diamagnetic heat flux is much larger than the perpendicular one, $\kappa_\wedge \gg \kappa_\perp$, but in practice the latter is never as small as this theory predicts because of additional turbulent transport. We therefore take the perpendicular and diamagnetic transport to be comparable and expand the temperature $T = T_0 + T_1 + \cdots$ accordingly. At zeroth order, we then find

$$\nabla \cdot \left(\kappa_\parallel \nabla_\parallel T_0\right) = R(T_0). \tag{2.4}$$

We assume that the magnetic field traces out topologically toroidal flux surfaces. If magnetic islands are present, these surfaces are not simply nested, but surfaces are still formed by the field lines unless the latter are chaotic due to island overlap. We assume that only a single chain of islands is present and that the field is thus integrable. (Even if it is not, similar considerations may apply thanks to the presence of so-called ghost surfaces (Hudson & Breslau 2008).) It is customary to define the flux-surface average $\langle \cdots \rangle$ of any function as the volume average of this function over the region between two neighbouring flux surfaces (Helander 2014). If ψ is some flux-surface label, i.e. a coordinate that is constant on each flux surface and varies smoothly between them, then the flux-surface average of the function $f(\boldsymbol{r})$ is thus

$$\langle f \rangle = \int_{dU} f(\boldsymbol{r})\, \mathrm{d}\boldsymbol{r} \Big/ \int_{dU} \mathrm{d}\boldsymbol{r}, \tag{2.5}$$

where $\mathrm{d}U$ denotes the region between the flux surfaces labelled by ψ and $\psi + \mathrm{d}\psi$, where $\mathrm{d}\psi \to 0$. It follows from Gauss' law that $\langle \nabla \cdot \boldsymbol{F} \rangle = 0$ vanishes for any single-valued vector field $\boldsymbol{F}(\boldsymbol{r})$ that is tangential to flux surfaces. The flux-surface average of (2.4) thus gives $\langle R(T_0) \rangle = 0$, which indicates that $R(T)$ should be relegated to higher order. The zeroth-order equation then becomes

$$\boldsymbol{B} \cdot \nabla \left(\frac{\nabla_\parallel T_0}{B} \right) = 0, \tag{2.6}$$

and it follows that T_0 cannot vary over flux surfaces, i.e. T_0 is some function of ψ alone that is determined by the higher-order equations. We thus proceed to the next order, where we find

$$\nabla \cdot \left(\kappa_\parallel \nabla_\parallel T_1 + \kappa_\wedge \boldsymbol{b} \times \nabla T_0 + \kappa_\perp \nabla_\perp T_0\right) = R(T_0). \tag{2.7}$$

A flux-surface average of this equation conveniently annihilates the first two terms, and thus produces an equation,

$$\langle \nabla \cdot (\kappa_\perp \nabla_\perp T_0) \rangle = R(T_0), \tag{2.8}$$

which, together with the boundary conditions, determines the lowest-order temperature $T_0(\psi)$. If the magnetic surfaces do not exist, as is the case for chaotic magnetic fields (Hudson & Breslau 2008), we note that the flux-surface average can be replaced by an appropriate average over ghost surfaces. As a result, the term representing parallel heat

https://doi.org/10.1017/S0022377824001727 Published online by Cambridge University Press

conduction is then not entirely annihilated. Since the loss function R is assumed only to depend on the temperature T, its flux-surface average is independent of the flux surface on which the radiation occurs, i.e. $\langle R(T_0)\rangle = R(T_0)$. Thanks to the large anisotropy of the heat conduction, we have thus reduced the original 3-D partial differential equation (2.1) to an ordinary 1-D differential equation. Indeed, if we supplement our flux-label coordinate ψ with two 2π-periodic coordinates (θ, φ) that specify the location within each magnetic surface, then (Hazeltine & Meiss 2003; Helander 2014; Helander, Hudson & Paul 2022; Paul *et al.* 2022)

$$\langle \nabla \cdot (\kappa_\perp \nabla_\perp T_0)\rangle = \frac{1}{V'(\psi)} \frac{\mathrm{d}}{\mathrm{d}\psi}\left(V'(\psi)\langle \kappa_\perp |\nabla\psi|^2\rangle \frac{\mathrm{d}T_0}{\mathrm{d}\psi}\right), \tag{2.9}$$

where

$$V'(\psi) = \int_0^{2\pi}\int_0^{2\pi} \frac{\mathrm{d}\theta\,\mathrm{d}\varphi}{(\nabla\psi\times\nabla\theta)\cdot\nabla\varphi} \tag{2.10}$$

is the derivative of the enclosed flux surface volume $V(\psi)$. Specifically, if we choose $V(\psi)$ as our flux-surface label instead of ψ, our equation (2.8) becomes simply

$$\frac{\mathrm{d}}{\mathrm{d}V}\left(\langle \kappa_\perp |\nabla V|^2\rangle \frac{\mathrm{d}T}{\mathrm{d}V}\right) = R(T), \tag{2.11}$$

where we have dropped the subscript on T_0. If $\kappa_\perp(T)$ is temperature-dependent, this dependence be eliminated from $\langle \kappa_\perp |\nabla V|^2\rangle$ though the definition of a new temperature

$$\tilde{T} = \int_0^T \kappa_\perp(T')\,\mathrm{d}T', \tag{2.12}$$

and a redefinition of $R(T)$.

In the 1-D conduction equation (2.11), the function $\kappa(V) = \langle |\nabla V|^2\rangle$ plays the role of an effective heat conduction coefficient, which encapsulates the influence of magnetic flux expansion on the perpendicular heat conduction. Our next step will be to calculate $\kappa(V)$ in a field with a single magnetic island chain. As we shall see, the fact that the topology of the magnetic field lines changes across the island separatrix implies a non-trivial topology of the set in which (2.11) is solved. Although this is an ordinary differential equation in terms of the independent variable V (the enclosed flux-surface volume), the latter does not have the usual topology of the real line.

3. Heat conduction equation near a magnetic island

3.1. *Magnetic island geometry*

Magnetic islands can arise in toroidal magnetic fields with nested flux surfaces in places where the rotational transform is a rational number. A resonant perturbation to the field-line Hamiltonian χ describing the field without the island in general produces such an island. If the perturbation only consists of a single Fourier harmonic, the perturbed field is described through a flux function similar to that of a pendulum Hamiltonian. From this analytical description of the island, it is possible to derive an expression for $\kappa(V)$ in terms of complete elliptic integrals.

A toroidal magnetic field can be described by

$$\boldsymbol{B} = \nabla\psi\times\nabla\theta + \nabla\varphi\times\nabla\chi_0. \tag{3.1}$$

If all flux surfaces are simply nested, then χ_0 is a function of ψ alone. We can thus write $\nabla\chi_0 = \iota(\psi)\nabla\psi$, where $\iota(\psi) = d\chi_0/d\psi$, and Clebsch coordinates can be defined by

https://doi.org/10.1017/S0022377824001727 Published online by Cambridge University Press

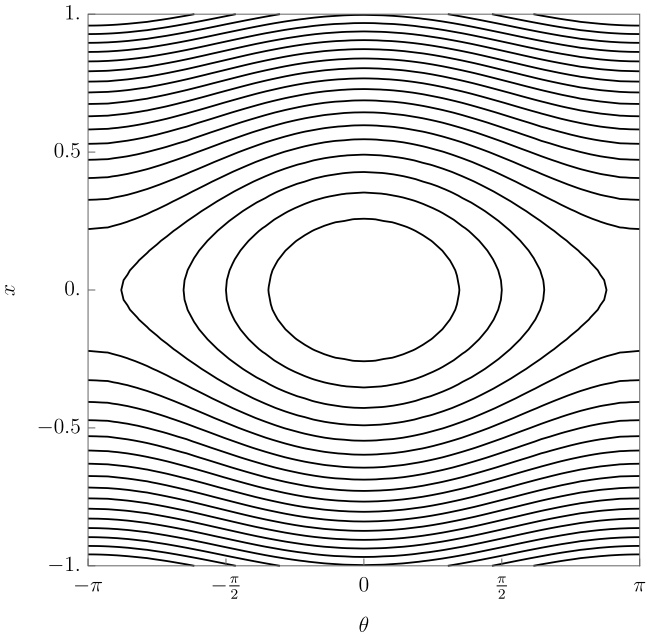

FIGURE 1. Contours of the magnetic flux χ for a magnetic field with an island and $\Omega = 1/4$.

$\alpha = \theta - \iota\varphi$, so that $\boldsymbol{B} = \nabla\psi \times \nabla\alpha$. The rotational transform $\iota(\psi)$ describes the number of poloidal turns per toroidal turn along a magnetic field line. Its derivative $\iota'(\psi)$ is known as the magnetic shear and describes how the rotational transform varies between flux surfaces. As already mentioned, magnetic islands on rational surfaces arise in response to a resonant perturbation $\delta\chi$ to the Hamiltonian system, and it is convenient for the description of a magnetic island to define a new effective Hamiltonian $\chi = \chi_0 + \delta\chi - \iota\psi$. The effective Hamiltonian facilitates the analysis by simplifying the system in a way similar to the description in Cary & Hanson (1991) and Lichtenberg & Lieberman (2013). Expanding the perturbation $\delta\chi$ in a Fourier series in the angular variables θ and φ, and keeping only one term in the expansion gives

$$\chi = \frac{1}{2}\iota' x^2 - F\cos\alpha, \tag{3.2}$$

where w measures the island width, x the deviation in ψ from the rational surface and $F = w^2\iota'/4$. For a detailed derivation see (Helander 2014) and (Hazeltine & Meiss 2003). The contours of χ are shown in figure 1. Next, we introduce the normalised island flux $m = \frac{1}{2}(\chi/F + 1)$:

$$m = \frac{1}{4\Omega^2}x^2 + \sin^2\vartheta. \tag{3.3}$$

Here we have introduced the island half-width $\Omega = (F/\iota')^{1/2} = w/2$ and the new angle $\vartheta = \alpha/2$. The normalised flux has the important property of lying between $0 < m < 1$ inside the island and $0 < 1/m < 1$ outside the island. For simplicity, we assume that unperturbed magnetic field is homogeneous and neglect any spatial variation of $|\nabla x|$, thus effectively considering the geometry of a plasma slab with a magnetic island.

https://doi.org/10.1017/S0022377824001727 Published online by Cambridge University Press

3.2. *Effective heat conductivity*

We proceed to determine the effective heat conduction coefficient in the magnetic island topology. From the 1-D heat conduction equation (2.11), it is clear that an expression for

$$|\nabla V|^2 = \left(\frac{\mathrm{d}V}{\mathrm{d}m}\right)^2 |\nabla m|^2, \tag{3.4}$$

needs to be determined from our normalised pendulum Hamiltonian (3.3). We use m as a flux-surface label and find, with the definition of the V' given earlier,

$$\frac{\mathrm{d}V}{\mathrm{d}m} = \begin{cases} \dfrac{4\Omega}{\sqrt{m}} K(m^{-1}), & m > 1 \\ 8\Omega K(m), & m < 1, \end{cases} \tag{3.5}$$

where K and E are complete elliptic integrals of the first and second kind, respectively. The argument may take any value between zero and unity. At the island O-point and far from the island $m \to 0$, whereas $m \to 1$ at the separatrix. To determine $|\nabla m|^2$ we express x^2 in (3.3) as a function of ϑ and m itself, and thus find

$$|\nabla m|^2 = \frac{1}{\Omega^2}\left(m - \sin^2\vartheta\right) + \frac{1}{4}\sin^2 2\vartheta. \tag{3.6}$$

Combining the expressions for $|\nabla m|^2$ and $\mathrm{d}V/\mathrm{d}m$ using $\sin^2 2\vartheta = 4(\sin^2\vartheta - \sin^4\vartheta)$, an expression for $|\nabla V|^2$ inside the island and outside the island can be found. The integrals in the flux surface averaging can again be reduced to combinations of K and E. For details on elliptic integrals see Byrd & Friedman (2012) and Gradshteyn & Ryzhik (2014). Proceeding in this fashion for $m < 1$ and $m > 1$, respectively, analytical expressions for the heat conduction coefficient κ can be found as a function of m. The result,

$$\kappa(m) = \begin{cases} \dfrac{16\Omega^2 K(m^{-1})}{3} & \\ \left[2\left(1-m\right)K(m^{-1}) + \left(2m - 1 + \dfrac{3}{\Omega^2}\right)E(m^{-1})\right] & m > 1, \\ \dfrac{8^2\Omega^2 K(m)}{3} & \\ \left[(m-1)\left(\dfrac{3}{\Omega^2} - 1\right)K(m) + \left(2m + \dfrac{3}{\Omega^2} - 1\right)E(m)\right] & m < 1, \end{cases} \tag{3.7}$$

can be combined into a single expression that is valid for all values of m:

$$\kappa(m) = \frac{1}{6}\left[\left(\frac{3}{\Omega^2} + 2m - 1\right)\frac{\mathrm{d}V^2}{\mathrm{d}m} + 4\left(m - m^2\right)\left(\frac{\mathrm{d}V}{\mathrm{d}m}\right)^2\right]. \tag{3.8}$$

As we shall see below, inside the island $\kappa(m)$ is well approximated by the first term in the square brackets, whereas both terms are required for an accurate description far outside the island. As is evident from the numerical plot given in figure 2, when the separatrix is approached from either side, κ goes to infinity because of the dependence on $K(m)$.

https://doi.org/10.1017/S0022377824001727 Published online by Cambridge University Press

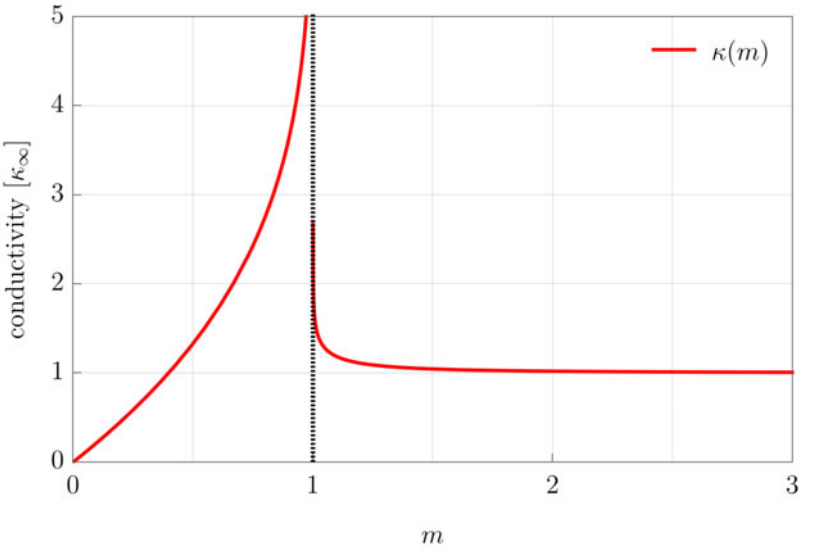

FIGURE 2. The equivalent 1-D heat conduction coefficient over the range of $0 < m < 3$. Outside the separatrix, κ quickly approaches the limiting value for $m \gg 1$. Here κ is normalised to κ_∞.

An analytical expression can also be given for $V(m)$,

$$V = \begin{cases} 8\Omega\sqrt{m}E(m^{-1}), & m > 1, \\ 16\Omega\left[E(m) + (m-1)K(m)\right], & m < 1, \end{cases} \tag{3.9}$$

which is plotted in figure 3. The enclosed flux surface volume for the pendulum Hamiltonian is related to the action integral $J = V/2\pi$, which is well known in Hamiltonian mechanics (Rechester & Stix 1979; Lichtenberg & Lieberman 2013).

At this point, it may be helpful to recapitulate the various coordinate transformations that have been performed. The unperturbed magnetic field (3.1) was originally written in general toroidal coordinates (ψ, θ, φ), and a magnetic island was added in a standard way through the introduction of the helical flux χ in (3.2). On the perturbed flux surfaces, which contain a periodic chain of magnetic islands, it proved useful to introduce the surface label m through (3.3) and the enclosed volume $V(m) =$ (3.9), in terms of which the effective heat conductivity (3.8) can be expressed.

For most choices of the radiation function $R(T)$, the differential equation (2.11) can only be solved numerically. To simplify the problem, we shall take $R(T)$ to be piecewise constant, in which case analytical progress is possible.

Regardless of the choice of $R(T)$, however, this equation has the interesting feature of operating in a domain of non-trivial topology. Although it is an ordinary differential equation, $T(V)$ is not to be understood as a function along a line but on the set with the topology shown in figure 5. The topology is similar to a rod with a cooling fin, where the latter corresponds to the interior of the island and the heat conductivity depends on the position along the rod and the cooling fin.

https://doi.org/10.1017/S0022377824001727 Published online by Cambridge University Press

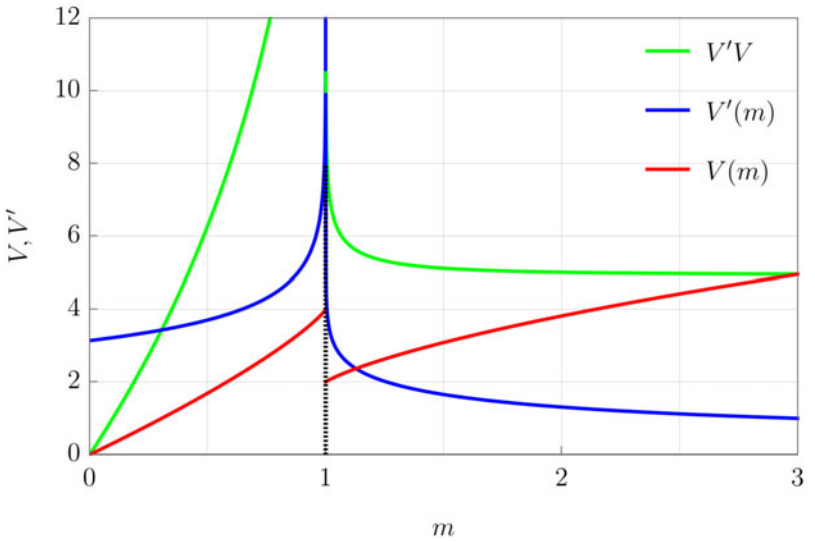

FIGURE 3. The enclosed flux-surface volume in and around the island and $V' = \mathrm{d}V/\mathrm{d}m$ with $\Omega = 1/4$. The discontinuity in V at the separatrix ($m = 1$) is due to the fact that there are two regions 'above' and 'below' the island for $m > 1$, each enclosing half of the total enclosed flux surface volume around the island. To understand the impact of competing V and V' terms, VV' is also shown.

3.3. *Limiting cases*

There are certain regions in which the heat conduction equation becomes particularly simple, namely, in the vicinity of the island O-point, at the separatrix and far away from the island. As one would intuitively expect, far from the island the equation reduces to an equation describing perpendicular heat conduction across flux surfaces without an island. Close to the O-point, the heat conduction equation is equivalent to that in an ellipse, and, as we shall see, the effective heat conduction coefficient κ reaches a maximum at the separatrix.

For the case far away from the island, we note that $m \gg 1$ and thus $\kappa \to \kappa_\infty = 4\pi^2$ becomes independent of V, as expected in a straight magnetic field. Equation (2.11) then reduces to

$$\frac{\mathrm{d}^2 T}{\mathrm{d}V^2} = R(T), \tag{3.10}$$

where we have absorbed $4\pi^2$ into $R(T)$.

In order to treat the region close to the O-point, we expand κ and V for small m, $\kappa(V) = 2\pi\Omega V(1 + 1/\Omega^2) + Om^2$, and note that (2.11) reduces to a heat conduction equation in elliptical geometry,

$$2\pi\Omega\left(1 + \frac{1}{\Omega^2}\right)\frac{\mathrm{d}}{\mathrm{d}V}\left(V\frac{\mathrm{d}T}{\mathrm{d}V}\right) = R(T). \tag{3.11}$$

The equation of the corresponding ellipse can be obtained by expanding equation (3.3) in ϑ, resulting in $4m = (x/\Omega)^2 + (2\vartheta)^2 + O\vartheta^3$. Thus, the ellipticity is given by the half-width of the island Ω, the radius of the ellipse is given through $r = 2\sqrt{m}$ and the enclosed volume near the O-point the enclosed flux surface volume dominates the heat conductivity.

https://doi.org/10.1017/S0022377824001727 Published online by Cambridge University Press

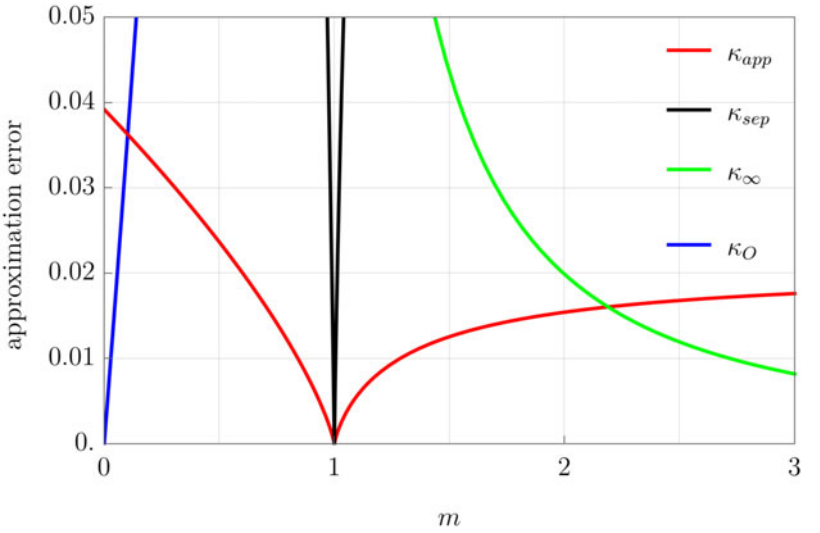

FIGURE 4. The deviation of the 1-D heat conduction coefficient from its asymptotic form in various limits. The expansion around the O-point and the separatrix (given as κ_O and $\kappa_{\rm sep}$), have very large errors farther away from their expansion point. While $\kappa_{\rm app}$ does not deviate more than 0.04 from $\kappa(m)$ in the relevant region in and around the island.

In the vicinity of the separatrix, κ can be expanded in $x \ll 1$ with $m = 1 - x$ inside the island and $m = 1/(1 - x)$ outside the island. In both cases, we find that the effective heat conduction coefficient is given by

$$\kappa = \frac{1}{6}\left(\frac{3}{\Omega^2} + 1\right) VV' + Ox, \tag{3.12}$$

where $V' = \mathrm{d}V/\mathrm{d}m$.

These approximations of the effective heat conductivity are asymptotically exact in the respective limits and less accurate elsewhere. The relative error $\left|\kappa_{\rm app} - \kappa\right|/\kappa$ is shown in figure 4. If the full expressions are used for the quantities V and V' in (3.12),

$$\kappa_{\rm app} = \frac{1}{6}\left(\frac{3}{\Omega^2} + 1\right) VV', \tag{3.13}$$

the resulting expression yields a remarkably good approximation everywhere in the domain, with an error less than a few per cent in figure 4. From this approximation, we conclude that the product VV' is the main contributing factor to the variation of the effective heat conductivity over the domain.

4. Variational principle

The effective heat conductivity across the magnetic field $\kappa(m)$ approaches infinity at the separatrix, which contradicts the ordering used to derive the 1-D heat conduction equation (2.11) in § 2. Accordingly, there is a boundary layer around the separatrix in which the temperature varies along the magnetic field and is not properly described by the ordinary differential equation (2.11). Instead, a 2-D treatment is necessary in this region, and one may ask whether this boundary layer may somehow affect the global properties of the

https://doi.org/10.1017/S0022377824001727 Published online by Cambridge University Press

solution. This seems unlikely since the boundary layer is narrow in the limit

$$\epsilon = \frac{\kappa_\perp}{\kappa_\parallel} \to 0, \tag{4.1}$$

but it is perhaps nevertheless of interest to demonstrate that the solution to (2.11) indeed converges to that of the original 2-D equation (2.1) in this limit.

An argument based on a variational principle can be constructed if the diamagnetic heat flux is neglected, $\kappa_\wedge = 0$. Then the trial function T that minimises the functional

$$D[T] = \int \left[(\nabla_\parallel T)^2 + \epsilon (\nabla_\perp T)^2 + \epsilon r(T) \right] \mathrm{d}\boldsymbol{r}, \tag{4.2}$$

with $r'(T) = 2R(T)/(\epsilon\kappa_\parallel)$, solves our original partial differential equation (2.1) if the temperature or its normal derivative is prescribed on the boundary. With these boundary conditions, (2.1) is satisfied if, and only if, $\delta D[T] = 0$. In particular, the function $T(\boldsymbol{r})$ that minimises the functional $D[T]$ satisfies this equation.

Equation (2.11) also corresponds to a variational principle, namely $\delta Q[T_0] = 0$, with

$$Q[T_0] = \int \left[\langle |\nabla V|^2 \rangle \left(\frac{\mathrm{d}T_0}{\mathrm{d}V} \right)^2 + k(T_0) \right] \mathrm{d}V, \tag{4.3}$$

where $k'(T_0) = 2R(T_0)/\kappa_\perp$. This functional is closely related to D: for functions $T(\boldsymbol{r})$ such that $\nabla_\parallel T_0 = 0$ they are proportional to each other, $D[T] = \epsilon Q[T]$. In other words, whereas (2.1) is satisfied by the function T that minimises $D[T]$ under the constraint that the boundary conditions are satisfied, the reduced equation (2.11) is satisfied by the function T_0 that minimises $D[T_0]$ under the additional constraint that $\nabla_\parallel T_0 = 0$. It follows that $D[T] \leq D[T_0]$.

Having established this variational principle, we now proceed to argue that the function $T(\boldsymbol{r})$ that solves (2.1) in the limit of large anisotropy in the heat conductivity is constant along magnetic-field lines, i.e.

$$\lim_{\epsilon \to 0+} \nabla_\parallel T = 0. \tag{4.4}$$

If this were not the case, it would be possible to find two points, $\boldsymbol{r}_P$ and $\boldsymbol{r}_Q$, on the same field line and a number $\tau > 0$ such that $T(\boldsymbol{r}_P) - T(\boldsymbol{r}_Q) > \tau$ for all sufficiently small values of $\epsilon > 0$. By continuity, the same would be true for points in a neighbourhood of $\boldsymbol{r}_P$ connected by field lines to a neighbourhood of $\boldsymbol{r}_Q$. Consider a 'flux tube' F connecting these neighbourhoods; then

$$D[T] \geq \int_F (\nabla_\parallel T)^2 \, \mathrm{d}\boldsymbol{r}, \tag{4.5}$$

where the right-hand side can be bounded from below (Helander *et al.* 2022). The bound is proportional to τ and depends on the geometry of the flux tube but is independent of ϵ, and it follows that $D[T]$ is similarly bounded from below in the limit $\epsilon \to 0+$.[1] But this leads to a contradiction since then $D[T] > D[T_0]$ for the function T_0 satisfying (2.11). We thus conclude that $T(\boldsymbol{r})$ cannot vary along flux tubes of non-vanishing volume in the limit $\epsilon \to 0+$, and that $T(\boldsymbol{r}) \to T_0(\boldsymbol{r})$.

[1] We assume that the cross-section of the flux tube does not shrink to zero in the limit of small ϵ, which would imply that the temperature difference τ is only maintained over an infinitesimally small volume.

https://doi.org/10.1017/S0022377824001727 Published online by Cambridge University Press

5. Heat transport in the equivalent 1-D geometry

We now proceed to solve the heat conduction equation (2.11) in a region containing the magnetic island and part of the surrounding plasma. We begin by appropriately normalising our variables and introducing a specific radiation function $R(T)$. This function is defined as follows:

$$R(T) = \begin{cases} R_0, & T_0 < T < T_1, \\ 0, & \text{otherwise}, \end{cases} \tag{5.1}$$

and ensures that radiation occurs only within a well-defined zone, bounded by the temperatures T_0 (cold side) and T_1 (hot side). The choice of this radiation function is driven by simplicity and aligns with the behaviour of line radiation from impurities in a typical plasma edge. The constant R_0 controls the radiation amplitude and is proportional to the impurity fraction and the square of the plasma density n_e^2.

There are several possibilities for the radiation front's position, as depicted in figure 5. The radiation zone can be situated on one side of the island, around the separatrix, below the island and between the separatrix and the O-point, as well as directly at the O-point. The region outside the island is taken to be bounded in one direction by a 'wall' with zero temperature and to extend some distance in the other direction, which in a tokamak or a stellarator would correspond to the far interior of the core plasma.[2] As already described, the topology of the 1-D set on which differential equation is to be solved is that of a rod with a cooling fin, see figure 5. Boundary conditions need to be prescribed at the wall, at infinity and at the O-point of the island. At the latter position, the heat flux must vanish, while the temperature is unconstrained. At the wall we impose the boundary condition $T = 0$, as the wall temperature is significantly lower than that of the plasma. At the other (hot) end of the domain, the incoming heat flux is prescribed.

It is convenient to normalise the variables in our 1-D heat conduction equation by writing

$$\hat{T} = \frac{T}{T_1}, \quad \hat{x} = \frac{V}{w}, \quad \hat{\kappa}(x) = \frac{\kappa(V)}{\kappa(\mathrm{d}w)}, \quad \hat{q}_{\mathrm{in}} = \frac{q_{\mathrm{in}}}{w}\kappa(\mathrm{d}w)T_1, \quad \widehat{R_0} = \frac{R_0 w^2}{\kappa(\mathrm{d}w)T_1}, \tag{5.2a–e}$$

where q_{in} denotes the incoming heat flux, i.e. the heat flux at x_d, and we have chosen $w = 4$ in the example shown above. Through the definition of $\hat{x}$, the enclosed flux-surface volume V is normalised to the island width w defined earlier, while in the definition of $\hat{\kappa}$ the heat conduction coefficient $\kappa(V)$ is normalised to its value at the hot end of the computational domain, which is situated at $\hat{x} = d$. Additionally, we introduce x_w as the position of the wall at the cold end of the domain.

When written in terms of these normalised variables, our heat conduction equation (2.11) and boundary conditions become

$$\frac{\mathrm{d}}{\mathrm{d}x}\left(\kappa(x)\frac{\mathrm{d}T}{\mathrm{d}x}\right) = R_0\left[\Theta(T-\tau) - \Theta(T-1)\right], \tag{5.3}$$

$$T(x_w) = 0, \tag{5.4}$$

$$T'(d) = q_{\mathrm{in}}, \tag{5.5}$$

[2]In the Wendelstein 7-X stellarator, the islands at the plasma boundary are normally positioned in such a way that they intersect the wall (divertor plates). Our expansion procedure is suited to deal with this situation, which involves substantial temperature variation along intersected field lines. We thus limit our discussion to a non-intersected island chain.

https://doi.org/10.1017/S0022377824001727 Published online by Cambridge University Press

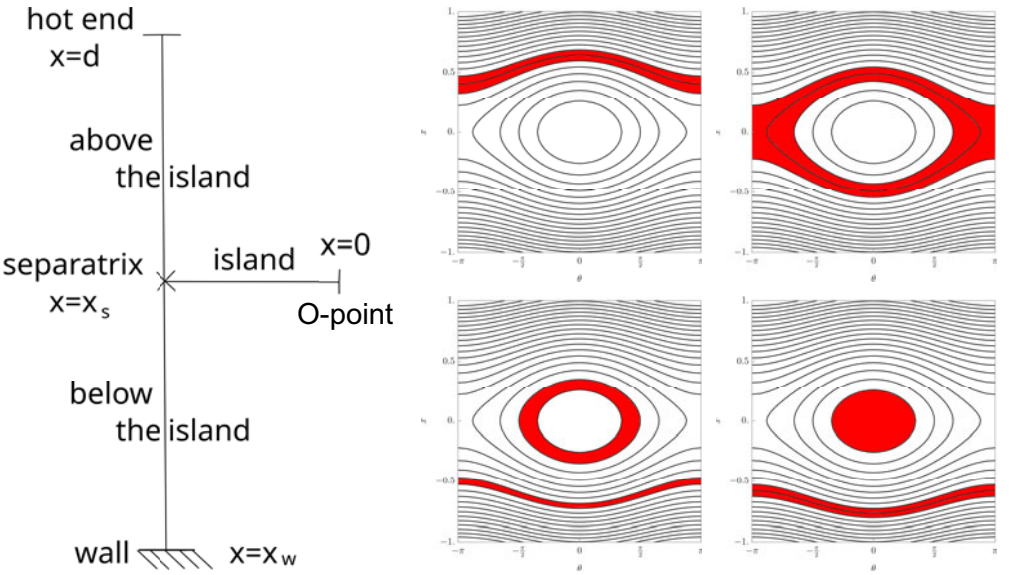

FIGURE 5. Equivalent 1-D topology of the heat conduction in a magnetic field with an island and the different positions of the radiation front. The topology is similar to a rod with a cooling fin. Here the interior of the island corresponds to the cooling fin and the heat conductivity depends on the position along the rod and inside the cooling fin. The radiation zone can be situated on one side of the island, around the separatrix, below the island and between the separatrix and the O-point, as well as directly at the O-point.

where Θ denotes the Heaviside step function, we have introduced the parameter $\tau = T_0/T_1$, and we have dropped carets over all quantities. By integrating this equation once, we find the relations

$$\frac{\tau}{q_{\text{out}}} = \int_{x_w}^{x_0} \frac{1}{\kappa(x)}\,\mathrm{d}x, \quad 1 = \tau + \int_{x_0}^{x_1} \frac{R_0(x-x_0)+q_{\text{out}}}{\kappa(x)}\,\mathrm{d}x, \quad T_{\text{up}} = 1 + q_{\text{in}} \int_{x_1}^{d} \frac{1}{\kappa(x)}\,\mathrm{d}x. \tag{5.6a–c}$$

It is evident from the dimensionless form of the equation that there are five free parameters, for instance q_{in}, τ, d, R_0 and x_w. We proceed by computing a number of illustrative solutions where four of these are held fixed while the remaining one is varied. We are particularly interested in seeing how the position and topology of the radiation zone then varies, which can be monitored by plotting x_0 and x_1, which are defined as the values of x at the cold and hot ends of the radiation belt, respectively, i.e. $T(x_0) = \tau$ and $T(x_1) = 1$. The total radiated power is $q_{\text{in}} - q_{\text{out}} = R_0(x_1 - x_0)$ where q_{out} represents the heat flux to the wall, and $x_1 - x_0$ is proportional to the radiating volume.

We do not endeavour to survey all possible solutions, but limit our attention to two different parameter scans in which τ and d are kept constant. In the first case, q_{in} is varied while $R_0 = 1$ is kept fixed, whereas in the second case we keep the incoming heat flux fixed and vary R_0. In addition, in the second case, solutions for different choices of x_w are shown as well. To highlight the influence of the island, we also present a solution using the normalised coordinates for a case without an island in the same normalised coordinates outside the island, with a constant heat conduction $\kappa(x) = 1$.

https://doi.org/10.1017/S0022377824001727 Published online by Cambridge University Press

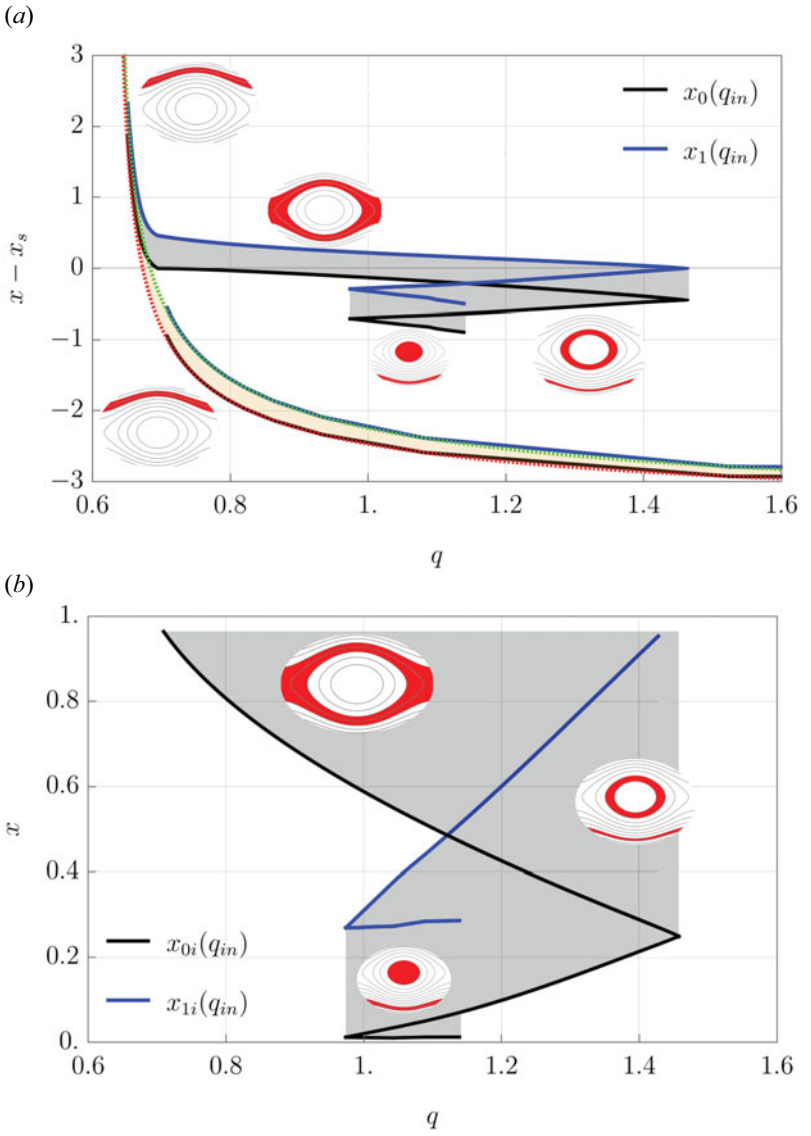

FIGURE 6. As the incoming heat flux $q_{\rm in}$ at $x = d$ is varied, the radiation zone moves around. Multiple positions are possible, both inside and outside the island, and the radiation zone may also straddle the separatrix. The curves show the location of the possible radiation zones (*a*) outside and (*b*) inside the island, and figures depict the geometry of the radiation zones in red. The wall is positioned at $x_w = -4$ the separatrix at $x_s = 0.5$, $R_0 = 1$ and $\tau = 0.8$. (*a*) Locations x_0 and x_1 defining the boundaries of the radiation band outside the island as functions of the incoming heat flux $q_{\rm in}$. Also shown as dotted curves are corresponding results for the case without an island. (*b*) Locations x_{0i} and x_{1i} defining the boundaries of the radiation band inside the island as functions of the incoming heat flux $q_{\rm in}$.

Results from the first parameter scan are shown in figure 6, where x_0 and x_1 are given as functions of the incoming heat flux $q_{\rm in}$. Figure 6(*a*) shows the position of the radiation zone outside the island, i.e. in the equivalent 1-D geometry between the wall and the

https://doi.org/10.1017/S0022377824001727 Published online by Cambridge University Press

hot end, while in figure 6(*b*) the radiation zone inside the island is shown. It is useful to note that $q_{\rm in}$ is not only the heat flux across the upper end of the domain but also represents the temperature gradient between the upper end and the radiation zone at x_1, where the incoming heat flux starts falling due to the radiated power and the temperature gradient therefore decreases. Thus, if $q_{\rm in}$ is large and the radiation zone is situated at the wall, the temperature gradient must be large. The temperature thus changes rapidly with x and reaches the value τ close to the wall, which is located at $x_w = -4$ in this example. In the limit $q_w \to \infty$ we thus expect $x_0 \to x_w$ and $x_1 \to x_w$, making the radiation band narrow and the radiated power fraction small. In other words, only a small amount of the incoming heat flux is radiated away, $q_{\rm rad}/q_{\rm in} \to 0$, and most of the incoming heat flux is deposited on the wall, $q_{\rm out} \simeq q_{\rm in}$. If $q_{\rm in}$ is reduced, the radiation zone recedes from the wall and approaches the island. Below a certain threshold, a multitude of possibilities arise: there is not one, but several solutions to the heat conduction equation, and radiation is possible both inside and outside the island.[3] Possibilities of radiation outside the island are illustrated in figure 6(*a*), which shows three pairs of curves. One observes a sudden jump in the sustainable heat influx $q_{\rm in}$ (see figure 6*a*) when radiation inside the island becomes possible. As the width of the radiation zone outside the island remains nearly constant in the vicinity of the island, all the changes in the heat flux are a result from changes inside the island. Only in this close vicinity of the island does the dependence of x_1 and x_0 differ substantially from the case without an island. When the radiation zone is close to the O-point, the radiation inside the island remains almost constant. Once the radiation in the island leaves the vicinity of the O-point, the radiation area increases (figure 6*b*) until the upper end of the radiation zone in the island x_{1i} reaches the separatrix. At this point, the greatest radiation intensity is achieved. Incidentally, in this position, the radiation zone also encloses the area with the greatest change in the enclosed volume, the separatrix. From this point onward, the radiation zone inside the island decreases with decreasing heat flux $q_{\rm in}$. When the radiation zone is situated above the island but in close proximity to it, an increase in the radiated heat flux compared with the case without the island is observed. Here, bifurcated solutions are observed, as multiple solutions are possible for a single $q_{\rm in}$.

It is evident from (3.8) that the rapid change $V'(m)$ in the enclosed volume makes κ particularly large close to the separatrix, implying a relatively small temperature gradient in this region and creating a greater capacity to sustain radiation. As mentioned earlier, the island opens up the possibility for multiple positions of the radiation front for the same $q_{\rm in}$. Figure 6(*a*) shows five different possibilities. Some of these may be thermally unstable, but we do not explore this question further.

We now proceed to the second parameter scan, where we keep $q_{\rm in}$ fixed but vary the radiation amplitude R_0, which mimics the effect of varying the impurity concentration in a fusion device at constant heating power (Stroth *et al.* 2022). The radiated power fraction $f_{\rm rad} = q_{\rm rad}/q_{\rm in}$ of course increases with increasing R_0 but does so in a non-trivial and interesting way. In figure 7, the radiation fraction $f_{\rm rad} = q_{\rm rad}/q_{\rm in}$ is shown as a function of R_0. To compare $f_{\rm rad}$ for different positions of the wall x_w, R_0 is normalised to the R_0 value at $f_{\rm rad} = 0.4$.

The cases without the island show a steady increase in the radiation fraction $f_{\rm rad}$ with R_0, connected to movement of the radiation zone. The cases with an island are very different. Most strikingly, $f_{\rm rad}$ is almost constant over a wide range of R_0. This range corresponds to situations in which radiation occurs from within the island and close

[3] Which one of the several solutions is actually realised depends on the prehistory of the system, which in other words exhibits hysteresis.

https://doi.org/10.1017/S0022377824001727 Published online by Cambridge University Press

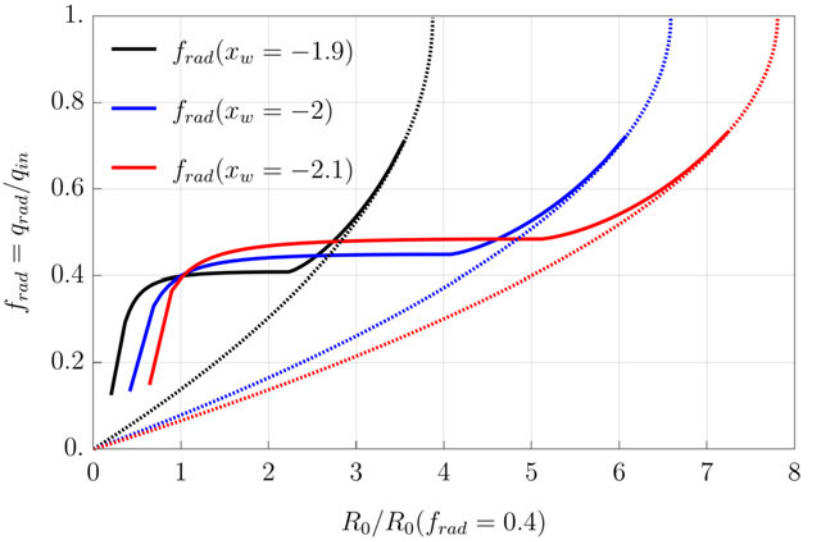

FIGURE 7. The radiation fraction f_{rad} as a function of R_0. Analytical solutions for a case without an island are also shown as dotted lines for comparison. The influence of position of the wall x_w and of the island on the radiation fraction is seen in the different position and gradients of the curves. The plot is normalised to $R_0(f_{\mathrm{rad}} = 0.4)$.

to the separatrix. It is thus evident that the presence of an island greatly affects the radiated power. The latter is much larger than in the case without an island, and the radiation has a tendency to linger in the vicinity of the separatrix. For small values of R_0, radiation mostly occurs close to the O-point and the radiation zone depends sensitively on R_0. If x_w is decreased, so that the island is brought closer to the wall, the heat flux domain deposited on the wall increases and the range in R_0 over which f_{rad} is constant decreases, as is evident from a comparison of the cases $x_w = 1.9$ and $x_w = 2.1$ in figure 7.

Finally, we explore the difference in effects resulting from the non-trivial topology induced by the island and the fact that the 1-D heat conductivity $\kappa(x)$ varies with x. To this end, we compare the temperature at the hot boundary of the region in two scenarios: firstly, a case featuring an island, as depicted in figure 6; secondly, a hypothetical scenario with identical topology but with constant heat conductivity $\kappa = 1$ throughout the domain (figure 8). This comparison shows that the ability to sustain high radiated heat fluxes in the vicinity of the island can mainly be attributed to the underlying topology: the additional volume made available through the island enhances the dissipation of thermal power. However, it is also evident that the broader range of potential radiation zone positions within the island does not emerge when κ is constant, indicating that part of the multiplicity is solely attributable to the spatial variation of $\kappa(x)$. The broader range of solutions stems from this variation within the island. For radiation between the separatrix and the O-point, the higher $\kappa(x)$ near the separatrix enables regions closer to it to radiate more power, as illustrated in figure 8. Similarly, the significantly lower heat conductivity near the O-point, combined with a radiation zone around it, is responsible for the third branch of solutions. This explains the additional branches in $T_{\mathrm{up}}(\kappa(x))$ shown in figure 8, as compared with the hypothetical scenario with identical topology but constant heat conductivity.

https://doi.org/10.1017/S0022377824001727 Published online by Cambridge University Press

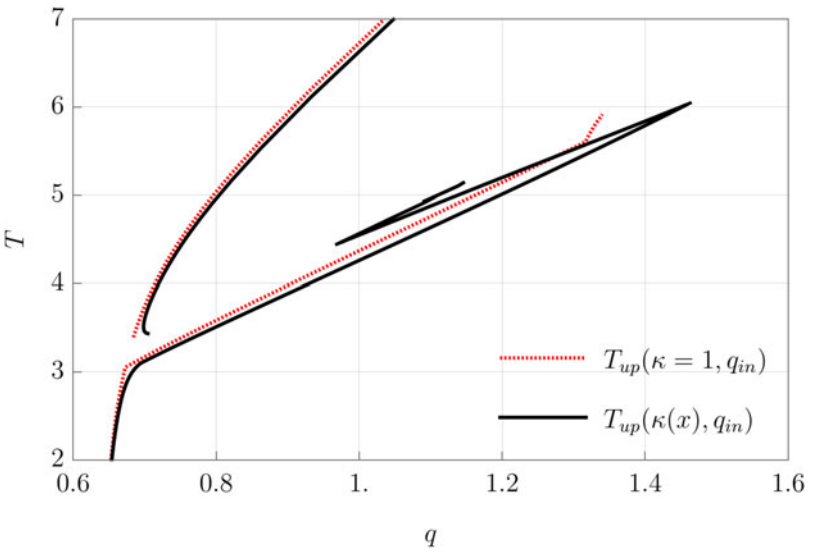

FIGURE 8. The temperature at the hot boundary of the region as a function of q_{in}. Shown are the curves for a case featuring an island in black and a hypothetical scenario with identical topology but with constant heat conductivity $\kappa = 1$ as a dotted lines for comparison.

6. Conclusion

In a plasma with very anisotropic heat conductivity, $\kappa_\parallel \gg \kappa_\wedge \sim \kappa_\perp$, heat conduction is much faster along the field than across it. As a result, the temperature tends to be constant along the field, and the steady-state heat conduction equation can be reduced to an ordinary differential equation describing conduction across magnetic flux surfaces, at least as long as the latter do not intersect the boundary. The effective cross-field heat conduction coefficient κ appearing in this equation encapsulates the net effect of the magnetic-field geometry and will thus depend on the position even if $\kappa_\perp$ and $\kappa_\parallel$ are constant. If a chain of magnetic islands is present, there is a change in topology across the separatrix, at which $\kappa \to \infty$. Moreover, although the reduced heat-conduction equation operates in one dimension, the topology becomes different from that of the real line, and corresponds to a rod with a cooling fin.

In practice, energy is not only conducted along the field but also lost through radiation. The radiation loss function varies with temperature, and the solutions of the resulting nonlinear equation exhibit bifurcations. These occur even in the absence of magnetic islands but become particularly interesting when they are present. If the simple model (5.1) is employed, so that radiation is emitted from a well-defined region, the latter can be located on either side of the island, inside the island or in multiple positions. As the incoming heat flux is varied, sudden transitions between these states are possible.

It is particularly important to note that, on the whole, a magnetic island enhances the plasma's overall capacity to radiate: the island indeed acts as a cooling fin. The total radiated fraction is higher when a magnetic island is present, and the radiation tends to linger in the island region as parameters such as the radiation amplitude or the incoming heat flux are varied. The plasma thus exhibits a tendency to radiate preferentially in the vicinity of the island, particularly around the separatrix. These features correlate qualitatively with observations in the island divertor of the W7-AS and W7-X stellarators (Feng *et al.* 2011, 2021), where, however, the magnetic geometry is more complicated

https://doi.org/10.1017/S0022377824001727 Published online by Cambridge University Press

than in the simple case analysed here, and the islands are normally intersected by divertor plates.

Acknowledgements

We sincerely thank the anonymous reviewers for their thoughtful and constructive comments, which greatly contributed to improving this paper. Their insightful suggestions and feedback were highly appreciated throughout the revision process.

Editor N. Loureiro thanks the referees for their advice in evaluating this article.

Funding

This work has been carried out within the framework of the EUROfusion Consortium, funded by the European Union via the Euratom Research and Training Programme (grant agreement no. 101052200 – EUROfusion). Views and opinions expressed are, however, those of the author(s) only and do not necessarily reflect those of the European Union or the European Commission. Neither the European Union nor the European Commission can be held responsible for them.

Declaration of interests

The authors report no conflict of interest.

REFERENCES

BRAGINSKII, S.I. 1965 Transport processes in a plasma. *Rev. Plasma Phys*. **1**, 205.

BYRD, P.F. & FRIEDMAN, M.D. 2012 *Handbook of Elliptic Integrals for Engineers and Scientists*. Springer.

CARY, J.R. & HANSON, J.D. 1991 Simple method for calculating island widths. *Phys. Fluids* B*: Plasma Phys*. **3** (4), 1006–1014.

FENG, Y., JAKUBOWSKI, M., KÖNIG, R., KRYCHOWIAK, M., OTTE, M., REIMOLD, F., REITER, D., SCHMITZ, O., ZHANG, D., BEIDLER, C.D., *et al.* 2021 Understanding detachment of the W7-X island divertor. *Nucl. Fusion* **61** (8), 086012.

FENG, Y., KOBAYASHI, M., LUNT, T. & REITER, D. 2011 Comparison between stellarator and tokamak divertor transport. *Plasma Phys. Control. Fusion* **53** (2), 024009.

GRADSHTEYN, I.S. & RYZHIK, I.M. 2014 *Table of Integrals, Series, and Products*. Elsevier Science.

HAZELTINE, R.D. & MEISS, J.D. 2003 *Plasma Confinement*. Dover Publications.

HELANDER, P. 2014 Theory of plasma confinement in non-axisymmetric magnetic fields. *Rep. Prog. Phys*. **77** (8), 087001.

HELANDER, P., HUDSON, S.R. & PAUL, E.J. 2022 On heat conduction in an irregular magnetic field. Part 1. *J. Plasma Phys*. **88** (1), 905880122.

HELANDER, P. & SIGMAR, D.J. 2005 *Collisional Transport in Magnetized Plasmas*. Cambridge University Press.

HUDSON, S.R. & BRESLAU, J. 2008 Temperature contours and ghost surfaces for chaotic magnetic fields. *Phys. Rev. Lett*. **100** (9), 095001.

JAKUBOWSKI, M., DINKLAGE, A., ENDLER, M., FENG, Y., KÖNIG, R., KRYCHOWIAK, M., PERSEO, V., REIMOLD, F., SCHMITZ, O., PEDERSEN, T.S., *et al.* 2021 Overview of the results from the divertor experiments at Wendelstein 7-X and their implications for steady state operation. *Nucl. Fusion* **61**, 106003.

KÖNIG, R., GRIGULL, P., MCCORMICK, K., FENG, Y., KISSLINGER, J., KOMORI, A., MASUZAKI, S., MATSUOKA, K., OBIKI, T., OHYABU, N., *et al.* 2002 The divertor program in stellarators. *Plasma Phys. Control. Fusion* **44** (11), 2365.

KRASHENINNIKOV, S.I. 1997 Two-dimensional effects in plasma radiation fronts and radiation front jumps in tokamak divertor plasmas. *Phys. Plasmas* **4** (11), 3741–3743.

KRASHENINNIKOV, S.I., BATISHCHEVA, A.A. & SIMAKOV, A.N. 1998 Radiation fronts in tokamak divertor plasmas. *Phys. Plasmas* **5** (6), 2297–2304.

LICHTENBERG, A.J. & LIEBERMAN, M.A. 2013 *Regular and Chaotic Dynamics*. Springer.

PAUL, E.J., HUDSON, S.R. & HELANDER, P. 2022 Heat conduction in an irregular magnetic field. Part 2. Heat transport as a measure of the effective non-integrable volume. *J. Plasma Phys*. **88** (1), 905880107.

RECHESTER, A.B. & STIX, T.H. 1979 Stochastic instability of a nonlinear oscillator. *Phys. Rev.* A **19**, 1656–1665.

STROTH, U., BERNERT, M., BRIDA, D., CAVEDON, M., DUX, R., HUETT, E., LUNT, T., PAN, O., WISCHMEIER, M., THE ASDEX UPGRADE TEAM, *et al.* 2022 Model for access and stability of the X-point radiator and the threshold for marfes in tokamak plasmas. *Nucl. Fusion* **62** (7), 076008.